Study of Speciation and Transport Properties for Different Compositions of Carbonates in Li 2 CO 3 – Na 2 CO 3 and Li 2 CO 3 – K 2 CO 3 Binary Systems at High Temperature in Molten State

Antonii Zhadan, Antoine Carof, Vincent Sarou-Kanian, Leire del Campo, Lionel Cosson, Rodolphe Vuilleumier, Mohammed Malki, Catherine Bessada

Study of speciation and transport properties for different compositions of carbonates in Li_2CO_3-Na_2CO_3 and Li_2CO_3-K_2CO_3 binary systems at high temperature in molten state

A. Zhadan[1], A. Carof[2], V. Sarou-Kanian[1], L. Del Campo[1], L. Cosson[1], R. Vuilleumier[3], M. Malki[1] and C. Bessada[1]*

AUTHOR ADDRESS

[1]Conditions Extrêmes et Matériaux: Haute Température et Irradiation, CEMHTI, UPR 3079 CNRS - Univ Orleans 45071 Orléans, France.

[2]Université de Lorraine, CNRS, LPCT, F-54000 Nancy, France

[3]PASTEUR, Département de Chimie, Ecole Normale Supérieur, PSL University, Sorbonne Université, CNRS, 75005, Paris, France.

KEYWORDS

Molten carbonates; high temperature; PFG NMR; electrical conductivity; CO_2; self-diffusion; molecular dynamics.

ABSTRACT

Molten alkali carbonates play a central role in carbon-capture technologies. To characterize the structural and transport properties, we gave used NMR, PFG NMR, electrical impedancemetry and molecular dynamics simulation. Different compositions in Li_2CO_3-Na_2CO_3 and Li_2CO_3-K_2CO_3 binary systems at 1003 K have been studied. The NMR measurements confirmed only the presence of anionic species CO_3^{2-} whatever the composition. Some structural evolution of K^+ and Li^+ cations around the oxygen was detected in the compositions Li_2CO_3-K_2CO_3. With the addition of K_2CO_3 in the carbonate mixture, the interaction between the charge carriers present in the liquid increases and results in a decrease of electrical conductivity.

Introduction

The different mixtures of alkaline carbonates are used as electrolytes in fuel cells[1] or to capture carbon[2] through their ability to dissolve CO_2.[3] Nevertheless, the speciation, the mechanisms of transport and of CO_2 dissolution are not yet well known. Which impedes the optimization of fuel cells and carbon-capture technologies.[4,5] There is not enough experimental data to clearly explain the physical properties of molten carbonates at high temperature.

In this study we explore the different compositions of carbonates in two binary systems Li_2CO_3-Na_2CO_3 and Li_2CO_3-K_2CO_3 at temperature over than 1000 K using Nuclear Magnetic Resonance (NMR)[6] to measure self-diffusion coefficients D[7] and chemical shifts[8], and Electrical Impedance Spectroscopy (EIS) to measure electrical conductivity.[9]

The study of molten carbonates is an experimental challenge, due to their high melting temperature,[10] their strong corrosiveness toward many materials,[11-12] their decomposition and their sensitivity to hydration. This expertise requires the development of new and efficient experimental setups. Taking into account all specific properties of molten carbonates, the optimization was implemented and described in our previous work.[8] Some of the authors

recently exploit this innovate experimental set-up to study the effect of temperature in different alkali carbonates at the eutectic compositions.[13] The impact of composition and alkali type is however lacking.

The first aim of this study is the description of the local structure according to the composition and the type of alkali metal. The second one is to explain in detail the conduction mechanism by coupling the NMR self-diffusion measurements with the electrical conductivity using the relation of Nernst-Einstein and factor Haven to explain in detail the conduction mechanism. We will verify if there is only an effect of the cation size or if other phenomena influence the electrical conductivity.

To analyse the speciation in molten carbonates, we have observed the ^{13}C and ^{17}O nucleus by NMR spectroscopy. The problem of these two isotopes is that they have very low natural abundance: 1.07% and 0.038 % respectively. For this reason, we used commercial powders of carbonates enriched by ^{13}C, that significantly reduced the time of acquisition. In the case of ^{17}O there is no commercial powders enriched by this isotope and we didn't succeed in its synthetises. We choose to work with ^{17}O natural abundance but with big number of acquisitions. The ^{23}Na, ^{7}Li and ^{39}K nucleus were also observed by NMR.

To measure self-diffusion coefficients, we have used high temperature pulse field gradient NMR (HT PFG NMR).[7] Previously, D were measured by radioactive tracers methods,[14] but with these experiments, it is not possible to study radioactive isotopes of chemical elements with a low half-time duration, such as lithium. PFG NMR is a selective technique and it does not require the use of radioactive isotopes. We can determine directly D over a wide diffusion range (10^{-9}-10^{-10} m^2/s).

For electrical conductivity measurements we have used the four-electrodes technique.[9] The principal advantages of the four-electrode method as compared to the classical two-electrode method are that the polarization effects are minimized, especially at high temperature and low frequencies. This method does not take into account the contribution of the platinum wires at the measured impedance, which is important for highly conductive solutions.[15]

Finally, we also performed molecular dynamics simulation to get detailed insights of the structure at a molecular level. In the field of molten salt and ionic liquid, molecular simulations have shown their ability to provide microscopic information on structure and thermodynamics,[16,17] or on dynamics and transport properties.[18–21] For instance, Salanne et al. explains how the network formation in LiBe-BeF_2 mixture induces a decoupling between viscosity and electrical conductivity with respect to Beryllium concentration.[22] In molecular dynamics simulations, the interactions between the atoms (i.e. energy and forces) are calculated *via* classical functions of the nuclear coordinates (namely, the force field) or by determining the electronic structure corresponding to the nuclear coordinates. If the latter is more accurate,[23] it demands more time and numerical resources and is usually limited to few tens of picosecond and few hundreds of atoms. The force field approach permits to simulate tens of thousands of atoms for several hundreds of nanoseconds but requires first a difficult step of parametrisation. Since the pioneering work of Janssen and Tissen,[24–26] several force fields were developed for molten carbonate at different temperatures, pressures and compositions.[17,27–31] They often focus on one or two alkali cations and are limited to a small range of temperature and pressure. We thus choose the force field recently developed by Desmaele et al. that allows to explore the microscopic properties of molten carbonate in a wide range of thermodynamical conditions (900-2000 K, 0-15 GPa).[29] We finally note a recent force field developed using machine learning with

a datasets generated from first-principles molecular dynamics,[32] this interesting strategy will deserve considerations in future works.

Experimental

Samples preparation

NMR experiments: the different Li_2CO_3-Na_2CO_3 and Li_2CO_3-K_2CO_3 compositions were prepared from dried powders Li_2CO_3 (99.998%), Na_2CO_3 (99.997%), K_2CO_3 (99.997%) ^{13}C enriched (99%) from Sigma-Aldrich. Sodium and potassium carbonate are sensitive to moisture, so all mixtures were prepared and stored in a glove box under dried argon. The salt was pressed in alumina (Al_2O_3) crucible. This crucible is then placed in a second magnesium oxide (MgO) crucible with a lid. The system of two crucibles has been described in a previous papers.[8, 13]

Electrical conductivity measurements: the same mixtures of carbonates, with no ^{13}C enrichment were prepared from Alfa Aesar and stored in glove box. The salt was then melted in an alumina crucible of 40 mm diameter and 60 mm height, under air, and then cooled down to be stored in an electric oven at 423 K to prevent any hydration of samples.

Materials characterization

NMR

To study materials at high temperature in liquid state by NMR spectroscopy, we used experimental device developed in CEMHTI-CNRS Orleans associated with NMR spectrometer Bruker AVANCE I NMR (magnetic field of 9.4 T) coupled with the system of heating by two lasers CO_2 (λ = 10.6 µm, 250 W).[33] The laser power is controlled by a computer for temperature control during the experiment. This heating system permits to heat the sample container (crucible) from top and bottom sides, for a good homogeneity of temperature inside the crucible during the experiment. For high temperature experiments we use an axial probe, initially

designed for liquid NMR which has been specially modified in the laboratory for lasers heating. It is a multi-nucleus static probe which can be tuned to the resonance frequency of the selected nucleus during high-temperature experiment.

^{7}Li, ^{23}Na, ^{39}K, ^{13}C and ^{17}O NMR measurements were performed for different compositions of binary systems Li_2CO_3-Na_2CO_3 and Li_2CO_3-K_2CO_3 under CO_2 atmosphere. For the references of chemical shifts, we used 1M aqueous solutions of LiCl, NaCl, KCl, silicon oil ($C_6H_{18}OSi_2$) and H_2O respectively. The silicon oil (PDMS) was used as a secondary reference equal to 0 ppm relative to tetramethylsilane (TMS). Using of PDMS is related to the design features of the high temperature NMR probe and volatility of TMS.

For measurements of self-diffusion coefficients we used HT PFG NMR technique[7,34] with a Bruker *Diff30* probe and a convection-free NMR pulse sequence proposed by Jerschow et al.[35] The diffusion coefficient, D was measured for ^{7}Li, ^{23}Na and ^{13}C for the same compositions and the same temperatures. We cannot measure the self-diffusion coefficients for ^{17}O and ^{39}K because of low natural abundance of oxygen-17 isotope (0.038%) and low Larmor frequency of ^{39}K (18.7 MHz).

Electrical conductivity

The electrical conductivity has been measured for the eutectic compositions in the binary systems Li_2CO_3-Na_2CO_3 and Li_2CO_3-K_2CO_3 in the temperature range from ~373 K to 1023 K, under CO_2 at 1 atm. For these measurements we used a four-probe technique[36] combined with a Solartron SI 1260 impedancemeter which working in the frequency range from 1 Hz to 1 MHz. This technique consists of four platinum electrodes where two plates applying a current flow between which two wires measure the voltage drop. This experimental setup is specially adapted for the measurements of electrical conductivity in molten salts at high temperature.[9,15] For the

analysis of molten alkali carbonates a special system of crucibles was created, already described in our previous article.[8] For the calibration of conductivity cell we have used 1M aqueous solution KCl at room temperature with a depth immersion of 8 mm of the electrodes in the melt.[37,38]

The four electrodes technique minimize the polarisation effects and does not take into account the contribution of the platinum wires at the measured impedance compare to the classical two electrode method.[39]

Details of simulations

Using classical (force field-based) molecular dynamics simulation, we studied the same binary systems as experiments: Li_2CO_3-Na_2CO_3 (with 40, 52, 60, 70, 80, and 90 % of Li), Li_2CO_3-K_2CO (with 40, 50, 62, 70, 80, and 90 % of Li) and the pure Li_2CO_3 at T = 1003 K, P = 1 atm. Each system consists of 5000 carbonates molecules and 10 000 cations (i.e., 30 000 atoms). Periodic boundary conditions are applied in all the directions.

In the initial configurations, the carbonate anions and cations are put on a regular grid. The systems were then equilibrated during 2 ns in the NPT ensemble and during 2 ns in the NVT ensemble. We used Nose-Hoover style barostat and thermostat with a time constant of 2 ps and 1 ps, respectively.[40–42] The production part is eventually done in the NVE ensemble for 10 ns, with all positions and velocities written every picosecond for the post-processing analysis (radial distribution function and diffusion). The simulations were performed with the LAMMPS software[43,44] and a velocity-Verlet algorithm is used to integrate the equations of motion. The time step is 1 fs.

We focus here on the intermolecular structure and dynamics -without reactivity- and we opted thus for a classical molecular dynamics simulation where energies and forces are calculated at

each time step using a force field function i.e., without electronic structure calculation. Among the existing force fields in the literature,[17,28,32] we chose the one recently developed by Desmaele et al. It shows a good comparison with experiments for thermodynamic, structural, and dynamical properties, as well as being easily transferable for all pure, binary and ternary mixtures of alkali-carbonate.[45] This force field consists of intermolecular pair interactions between alkali atoms and alkali and oxygen atoms, with a van der Waals and an electrostatic terms, and intramolecular interactions within the carbonate anion. The long-distance part of the electrostatic interactions is computed using the standard Ewald summation technique,[46] with a cut-off of 12 Å and an accuracy of 10^{-5}.

Results and discussion

^{23}Na, ^{7}Li, ^{39}K and ^{13}C, ^{17}O NMR spectra

For the binary systems Li_2CO_3-Na_2CO_3 and Li_2CO_3-K_2CO_3 the measurements of ^{23}Na, ^{7}Li, ^{39}K, ^{13}C and ^{17}O NMR chemical shifts were realised at 1003 K. We studied the mixtures above 40 mol% of Li_2CO_3. For compositions with a lower Li_2CO_3 content, the melting temperature is greater than 1003 K which can provoke a parasitic reaction with alumina crucible.[12]

For the binary system Li_2CO_3-Na_2CO_3 the results are presented in figure 1(a). For the different compositions of this system we don't see any significant variation of chemical shifts. For ^{23}Na and ^{7}Li the chemical shifts are always around 0 ppm ^{13}C and ^{17}O chemical shifts show also an almost constant value around 172 ppm for the two nuclei corresponding to the presence of CO_3^{2-}[47,48] for all compositions.

In the case of Li_2CO_3-K_2CO_3 binary system (figure 1(b)) the chemical shifts of cations ^{7}Li, ^{39}K do not change with the amounts of Li_2CO_3 and are equal to 0 ppm. The ^{13}C chemical shift tend towards the same value (172 ppm) whatever the composition. In the case of oxygen, a quasi-

linear relationship is obtained with the addition of potassium carbonate. The evolution of ^{17}O chemical shift from 187.5 ppm to 172.3 ppm, indicates a change in the environment around the oxygen. The chemical shifts of ^{13}C and ^{17}O measured are characteristic for the CO_3^{2-}.[47,48]

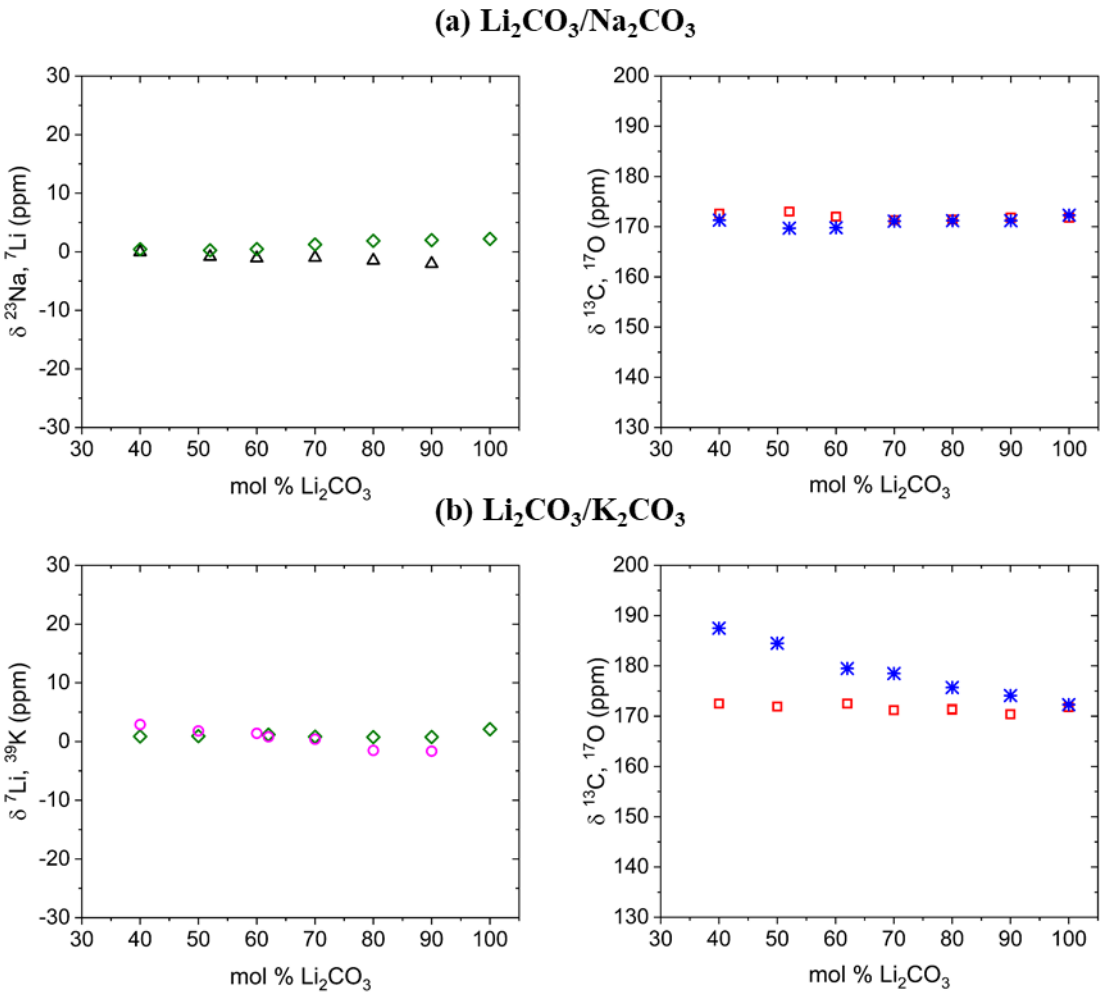

Figure 1. Evolution of ^{23}Na (black triangle), ^{7}Li (green titled square), ^{39}K (purple square) and ^{13}C (red square), ^{17}O (blue asterisk) chemical shifts in the different compositions in binary systems Li_2CO_3-Na_2CO_3 and Li_2CO_3-K_2CO_3 at 1003 K.

To better understand the environment around the oxygen in the two binary systems we have calculated the radial distribution function (RDF) from the molecular dynamics simulation. Figure

2 presents the RDFs between the oxygen atom and the different cations for the different compositions of the binary systems Li_2CO_3-Na_2CO_3, Li_2CO_3-K_2CO_3, and for the pure Li_2CO_3.

In Li_2CO_3-Na_2CO_3, the RDF O-Li and O-Na are characterized by a first peak relatively intense, situated at 2.85 Å and 3.26 Å, respectively. The peak is followed by a first minimum that delimits the first solvation shell around the oxygen. However, this minimum is very shallow meaning that the energy barrier to leave the shell is small. The medium range distance (4-5 Å) displays a second shell and the RDF converges to 1 in the long-range distance.

When the content of Li increases, the RDF O-Li and O-Na remain almost unchanged. We simply note a slight decrease of the height of the first peak, which means that the interaction strength between the oxygen and the cations diminishes. The position of the peak and the remaining part of the RDFs are independent of the compositions. We conclude that the microstructure of Li_2CO_3-Na_2CO_3 is unaffected by the content of Li.

We also calculate the number of cations (Li, Na or K) surrounding the oxygen atoms,

$$n_{cat}(R)=\rho_{Li}\int_0^R d\,r4\pi r^2 g_{Li\text{-}O}(r)+\rho_{Na}\int_0^R d\,r4\pi r^2 g_{Na\text{-}O}(r) \quad (1)$$

where ρ_{Li} is the concentration of Li, ρ_{Na} is the concentration of Na. Figure 2(c) displays this number for the different compositions. The number of cations increases from 0 to 4 between 1.9 and 3.2 Å. That increase is steeper for the systems with a higher content of Li, as Li is closer than Na to the oxygen atom. At 3.2 Å, the numbers of cations almost coincide for all the compositions, before they start diverging and increasing again.

We applied the same analysis to the microscopic structure in the binary Li_2CO_3-K_2CO_3 (Figure 2 (d-e)). The positions of the first peak are 2.85 and 3.67 Å for O-Li and O-K, respectively. The position of the O-Li peak is identical in both Li_2CO_3-K_2CO_3 and Li_2CO_3-Na_2CO_3, but its height is much higher in Li_2CO_3-K_2CO_3. On the other hand, the height of first O-

K peak is smaller than the O-Na peak. The decay of first peaks height (for both O-Li and O-K) with Li content is more pronounced than for Li_2CO_3-Na_2CO_3. This structural difference is also noticeable for the second minima of the RDF which remains almost unchanged for Li_2CO_3-Na_2CO_3 but are clearly composition-dependant in Li_2CO_3-K_2CO_3. To highlight these differences, we consider again the number of cations around the oxygen atom (using Equation 1 where we replace Na with K). As it is shown in Figure 2(f), the shape of the cations number is similar to the one in Li_2CO_3-Na_2CO_3 but there is no convergence of all compositions at a given radius.

The RDFs shown here are equivalent to the one presented in the literature of molten carbonate simulations for the same pressure and a similar temperature range.[28,29,31,32] In particular, the previous studies have also noted the invariance of the first peak positions for the RDF O-cations with respect to the composition.[31,32] Only a large increase of pressure is able to decrease the O-cations distance in the first solvation shell.[17,28]

To get more insights into the microscopic solvation structure around the carbonate anion, we also extracted the cation 3D-densities. Fig. 3 presents the Li (orange), Na (blue) and K (purple) 3D-densities around a carbonate anion for four different compositions: 60% Na, 10% Na, 60% K, and 10% K. The final densities display the same D_{3h}-symmetry as the carbonate anion. In all the four compositions, the maxima of densities of Li are similar: they form six “lobes”, three situated in front of the oxygen atoms and three situated in the bisector of the OCO angle. The K densities are similar for both compositions 60 % K and 10% K, they are situated in the three bisectors of the OCO angle, and at a larger distance than the Li (in accordance with the change of position of the first O-cation RDF peak). The sodium cations densities depend on the compositions: at high Na content (60 % Na), the density forms the same six lobes as Li but

slightly further away; at low Na content (10 %), the density only concentrates in the same three lobes as the K-density.

The MD simulations indicates that increasing of content of Li modifies both the composition of the first solvation shell around the carbonate anion and the microscopic organisation. In the case of Li_2CO_3-Na_2CO_3, the replacement of Na with Li in the first solvation shell does not change the chemical shift of the ^{17}O (Figure 1). We can relate this to the similar intermolecular O-cation distance (2.85 Å for Li, 3.26 Å for Na) and to the convergence of cation numbers in the first solvation shell (Figure 2(c)). On the other hand, K is more distant than Li to the oxygen atom (3.67 Å vs 2.85 Å). When Li replaces K in the first solvation shell, there is no convergence of cation numbers, and we observe a shift in the chemical shift of ^{17}O (Figure 1).

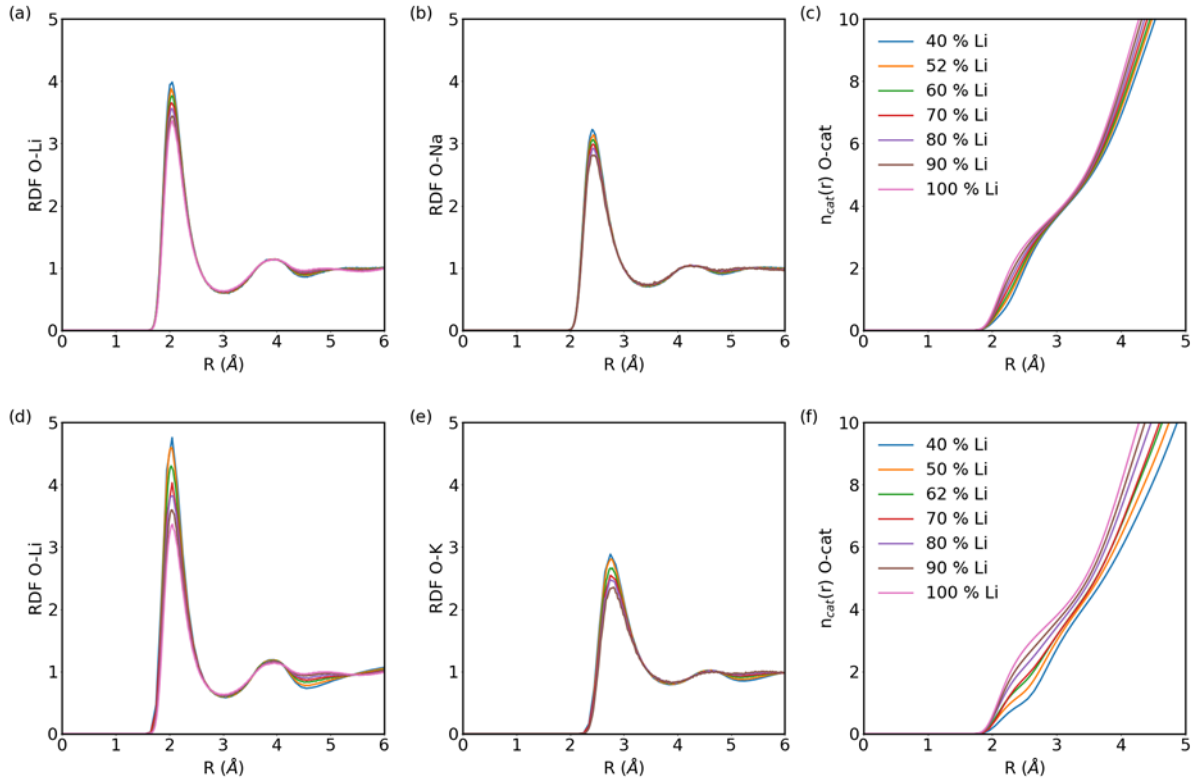

Figure 2. Microscopic structure from molecular dynamics simulations. (a)-(b) Radial distributions function between the oxygen atom and the cations in the mixture Li_2CO_3-Na_2CO_3

for different compositions and in the pure Li_2CO_3. (c) Number of cations (Li or K) at a distance R of an oxygen atoms (Equation 1). (d-f) Same as before but for the mixture Li_2CO_3-K_2CO_3.

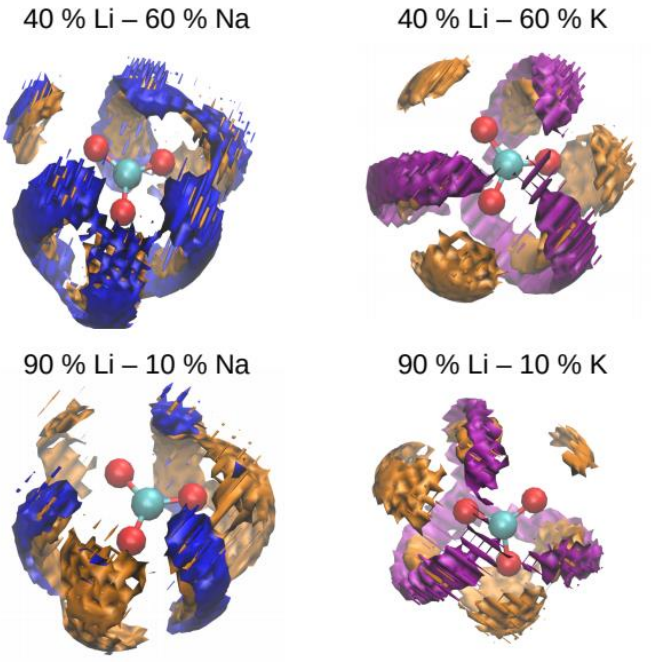

Figure 3. Microscopic solvation structure from molecular dynamics simulations: 3D-densities of the cations for 4 different compositions. Orange density: Li, blue density: Na, purple density: K.

Transport properties

^{23}Na, ^{7}Li and ^{13}C PFG NMR

The values of the self-diffusion coefficients measured by HT PFG NMR in the different carbonate mixtures Li_2CO_3-Na_2CO_3 at 1003 K are presented in figure 4 and compared with the experimental values obtained by Spedding et al.[49] at 1123 K by radiotracer. We also present the self-diffusion coefficient calculated from the molecular dynamics simulation, using the long-time linear regime of the mean square displacement.

From the experimental results of this work, a quasi-constant values of the auto-diffusion coefficients for the CO_3^{2-} anions and Li^+ and Na^+ cations are observed. Spedding et al.[49] observed

a maximum in diffusion of CO_3^{2-} and Na^+ ions in Li_2CO_3-Na_2CO_3 (52:48 mol%) composition but at higher temperature (1123 K). This difference can be explained by a bigger temperature interval from the melting temperature of eutectic composition. The simulation results compared well with the experimental values, showing quasi-constant values for different composition.

We note the measurement of the auto-diffusion coefficients for the CO_3^{2-} anions may be affected by the dissociation of CO_3^{2-} into CO_2. For instance, the auteurs Janz, G. J. and Lorenz M. R.[50] explained that high tracer diffusivities found for the CO_3^{2-} ion is based on the assumption that the C^{14} diffusion in the carbonate melt may easily be superimposed and thus falsified by transport of gaseous $C^{14}O_2$ after liquid/gas exchange. In this work using PFG NMR technique and a certain experimental set-up, we do not notice however any effect of CO_2 on diffusion measurements, which gives a more reliable results for $D(CO_3^{2-})$.

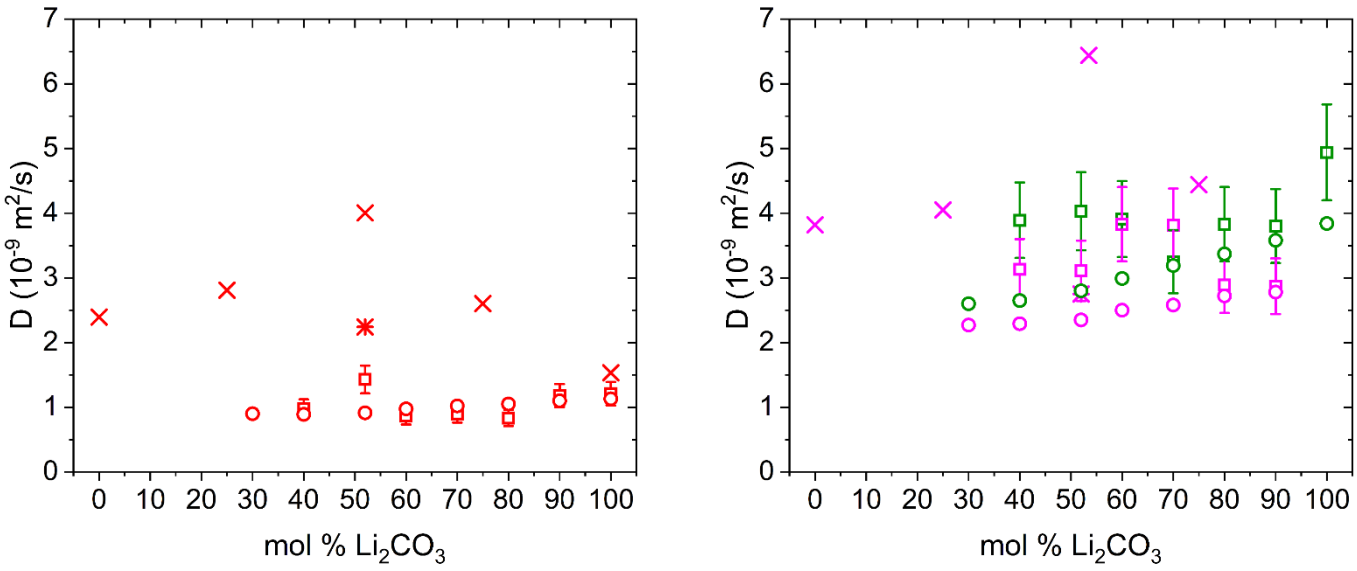

Figure 4. Self-diffusion coefficients of Li^+ (green squares), Na^+ (rose squares) and CO_3^{2-} (red squares) in Li_2CO_3-Na_2CO_3 mixtures depending on the composition (mol% Li_2CO_3) at 1003 K, compared with Spedding et al.[49] at 1123 K (crosses) and simulation results at 1003 K (circles).

For Li^+ and Na^+ cations, the self-diffusion coefficients measured are almost identical. For CO_3^{2-} anion the movement is lower than that of cations, that can be explained by its bigger size.

The self-diffusion coefficients of CO_3^{2-} and Li^+ were measured at different compositions in the binary system Li_2CO_3-K_2CO_3 at 1003 K. Obtained experimental results were compared to the simulated data and values obtained by Spedding et al.[51] at 1003 K. The self-diffusion coefficients for different Li_2CO_3-K_2CO_3 mixtures do not show any dependence with composition.

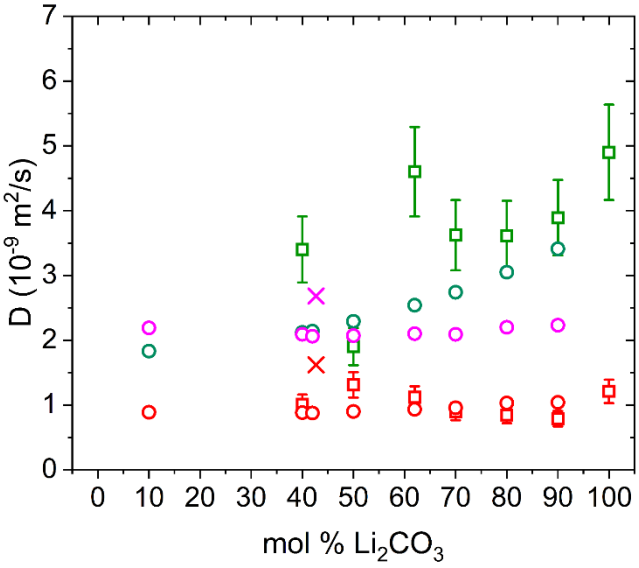

Figure 5. Self-diffusion coefficients of Li^+ (green squares) and CO_3^{2-} (red squares) in Li_2CO_3-K_2CO_3 mixtures depending on the composition (mol% Li_2CO_3) at 1003 K, compared with Spedding et al.[51] at 1003 K for K^+, CO_3^{2-} (crosses) and simulation results at 1003 K (circles).

From comparison of the self-diffusion coefficients of alkali ions from two binary systems Li_2CO_3-Na_2CO_3 and Li_2CO_3-Ka_2CO_3, it becomes clear that diffusion decreases with increasing ionic radius, which in turn effects on the electrical conductivity of molten carbonates as previously noticed by Näfe.[52]

Discussion

The measurement of self-diffusion coefficients by HT PFG NMR technique, allowed calculating the "ideal" or Nernst-Einstein conductivity (σ^{NE}) using equation 2 for each species present in molten carbonate.

$$\sigma^{NE} = \frac{q^2}{k_B T V} \sum_s N_s z_s^2 D_s \quad (2)$$

where q is the elementary charge, s concerns the conduction species (Li^+, Na^+, K^+ and CO_3^{2-}), N_s is the number of s ions contained in the volume V, z_s the conduction charge and D_s the experimental self-diffusion coefficients for the chemical species s. To calculate the molar volume V, we used the densities provided by Kojima et al.[53] and Janz et al.[54]

From the chemical shifts measured in Li_2CO_3-Na_2CO_3 system, we can evidence only Li^+, Na^+ and CO_3^{2-} species whatever the composition. For each ion we have calculated the ideal conductivity at 1003 K for different mixtures Li_2CO_3-Na_2CO_3 (table 1).

Table 1. Ideal conductivities σ^{NE} calculated for Li^+, Na^+ et CO_3^{2-} ions in different compositions Li_2CO_3-Na_2CO_3 at 1003 K.

%Li_2CO_3	**$\sigma^{NE}_{Li^+}$ (S/m)**	**$\sigma^{NE}_{Na^+}$ (S/m)**	**$\sigma^{NE}_{CO_3^{2-}}$ (S/m)**
40	72.2	87.1	90.6
52	101	71.7	137
60	116	75.6	85.2
70	116	58.2	91.5
80	159	30.0	86.9
90	182	15.3	126
100	273	0	134

From this calculations, we observe that σ^{NE} of the carbonate anions is less than the sum of the conductivities for the two cations Li^+ and Na^+ whatever the composition. These results confirm again the behaviour that we have already observed in the eutectics compositions of carbonates.[13] The electric current is mainly carried by the smallest ions – cations. The contribution to ideal conductivity by Li^+ and Na^+ cations changes with composition: by increasing Li_2CO_3 content, the conductivity $\sigma^{NE}_{Na^+}$ decreases and $\sigma^{NE}_{Li^+}$ on contrary increases, like $\sigma^{NE}_{CO_3^{2-}}$. We note in particular an excess value at the eutectic composition Li_2CO_3-Na_2CO_3 (52:48 mol%) due to a high value of the CO_3^{2-} self-diffusion coefficient.

We have calculated the total ideal conductivities σ^{NE} from equation (3) for each composition and then we have compared these ideal conductivities with the experimental electrical conductivities σ measured by impedancemetry.

$$\sigma^{NE} = \sum_s \sigma_s^{NE} \quad (3)$$

Knowing the electrical conductivities, we calculated factor Haven (H) from the equation 4 to see if the interaction between the ions changes with the composition during the charge transport.

$$H = \sigma^{NE}/\sigma \quad (4)$$

The evolution of H factor could explain the change of the complexation in the molten system. The Haven ratio (H) reflects the effect of interactions between the ions on the conductivity of composition. If H is significantly different from 1, it means that there are some interactions between the ions (cations or anions), and the charge carriers cannot move “freely” in molten salt. To calculate the H factors for the different compositions we have used the experimental conductivities (σ) measured by Kojima et al.[39] The results are reported in table 2.

Table 2. Comparison of the ideal conductivities σ^{NE} calculated from the self-diffusion coefficients measured by HT PFG NMR[7,34] with the experimental conductivities measured by Kojjima et al.[39] (Li_2CO_3-Na_2CO_3)

%Li_2CO_3	σ^{NE} (S/m)	σ (S/m) (Kojima et al.[39])	H
40	249.9	237.4	1.1
52	309.7	253.8	1.1
60	276.8	278.5	1
70	265.7	291.4	0.9
80	275.9	327.1	0.8
90	323.3	365.4	0.9
100	407	409.3	1

Figure 6 shows the evolution of H with composition in the Li_2CO_3-Na_2CO_3 system at 1003 K. The red square in figure 6 shows the H factor calculated from our conductivity measurements. The Haven ratio is very close to 1 for the different mixtures, due to very low interactions between the ions in the molten salts during charge transport whatever the composition. Speciation does not change either and only Li^+, Na^+ cations and CO_3^{2-} are present In the theory of Janz, G. J. and Lorenz M. R.[50,] his result would correspond to an electrical conductivity mechanism induced by the free ion, i.e. that molten carbonates are completely ionized. In Li_2CO_3-Na_2CO_3, the cations Li^+, Na^+ and the anions CO_3^{2-} are the main kinetic entities contributing to electrical conductivity. This picture coincides with the solvation structure we characterized by simulation: the first solvation shell is only weakly delimited, as the first minimum in the RDF O-Li and O-Na is shallow for all compositions in Figure 2.

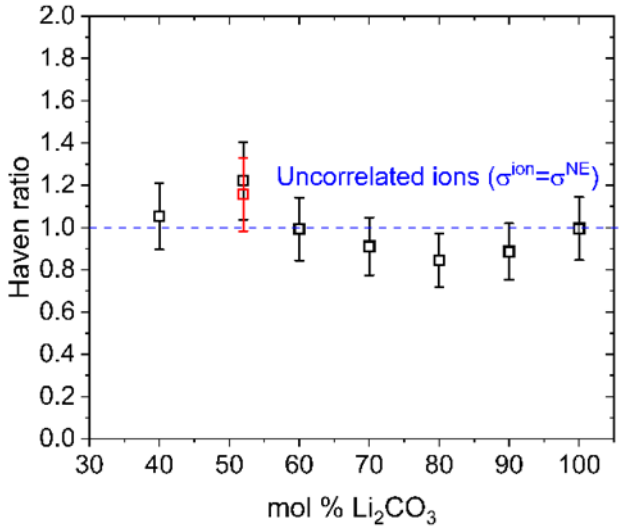

Figure 6. Factor Haven at 1003 K in the Li_2CO_3-Na_2CO_3 system. The black squares are obtained from the conductivities measured by Kojima et al.[39] and the red square (eutectic) from our own conductivity measurements.

As for the previous system, we have calculated the ideal conductivities for the different charge carriers in the Li_2CO_3-K_2CO_3 system.

The ideal conductivity for the potassium cation $\sigma^{NE}_{(K^+)}$ was calculated from the simulated results. To calculate the molar volume V, we used the densities provided by Janz et al.[55] The calculated ideal conductivities σ^{NE} are presented in table 3.

The value of the $\sigma^{NE}_{CO_3^{2-}}$ is less than the sum of Li^+ and K^+ regardless of the lithium carbonate content, as in the binary system Li_2CO_3-Na_2CO_3. This explains that the electric current in the Li_2CO_3-K_2CO_3 system is mainly carried by the smallest ions (cations). The ideal conductivity ratio of Li^+ and K^+ changed with composition. With the increase of Li_2CO_3 content, $\sigma^{NE}_{(K^+)}$ decreases and $\sigma^{NE}_{Li^+}$ increases. For $\sigma^{NE}_{CO_3^{2-}}$ there is no clear dependency with the composition. Due to the high value of the CO_3^{2-} self-diffusion coefficient in the Li_2CO_3-K_2CO_3 (50:50 mol%) composition, the $\sigma^{NE}_{CO_3^{2-}}$ is higher, and $\sigma^{NE}_{Li^+}$ is smaller due to the low $D(Li^+)$ value.

Table 3. Ideal conductivities σ^{NE} calculated for the Li^+, K^+ et CO_3^{2-} ions in different compositions Li_2CO_3-K_2CO_3 at 1003 K.

%Li_2CO_3	$\sigma^{NE}_{Li^+}$ (S/m)	$\sigma^{NE}_{K^+}$ (S/m)	$\sigma^{NE}_{CO_3^{2-}}$ (S/m)
40	51.9	47.9	77.1
50	38.8	41.63	105
62	124	34.5	96.9
70	114	28.3	81.2
80	139	21.2	81.3
90	180	11.5	80.8
100	273	0	134

With ideal conductivities shown in table 3 we can calculate total ideal conductivities and compare with our experimental results and Kojima et al.[56] We show this comparison in table 4.

Table 4. Comparison of the ideal conductivities σ^{NE} calculated from the self-diffusion coefficients measured by HT PFG NMR[7,34] with the experimental conductivities measured by Kojjima et al.[39] (Li_2CO_3-K_2CO_3)

%Li_2CO_3	σ^{NE} (S/m)	σ_1 (S/m) This work	$H = \sigma^{NE} / \sigma_1$	σ_2 (S/m)[39]	$H = \sigma^{NE} / \sigma_2$
40	177	137.2	1.3	139.5	1.3
50	196	-	-	149.9	1.3
62	255	186.1	1.4	167.6	1.5
70	224	-	-	188.6	1.2
80	241	-	-	232.8	1
90	272	-	-	293.3	0.9
100	407	-	-	409.3	1

The Haven factors from table 4 are presented in figure 7. For the compositions where the concentration of Li_2CO_3 is lower than 70% the H are always greater than one.

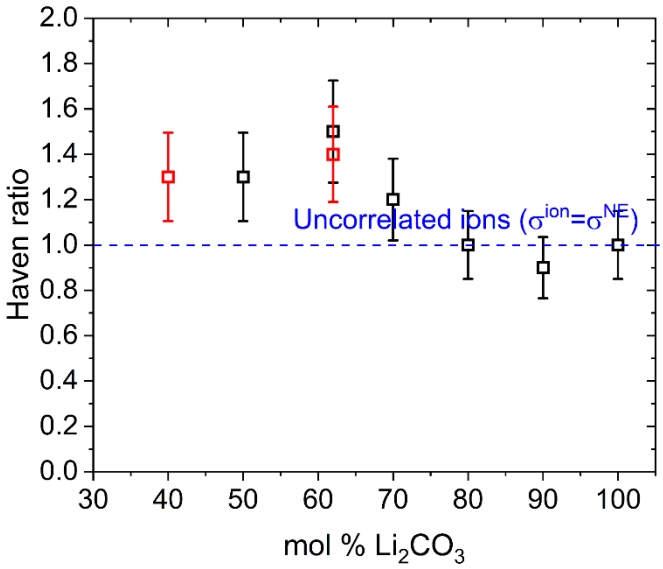

Figure 7. Factor Haven at 1003 K in the Li_2CO_3-K_2CO_3 system. The black squares are obtained from the conductivities measured by Kojima et al.[39] and the red squares (eutectic) from our own conductivity measurements. (For the composition Li_2CO_3-K_2CO_3 (40:60 mol%) the red and black squares superimposed)

High values of H can be explained by an increase of the interactions between the ions with additions of K_2CO_3. In other words, the electrostatic interactions globally attenuate the mobility of the charge carriers in the molten salt, which reducing the electrical conductivity of these compounds compared to the values of the ideal conductivity (free movement of ions). Janz, G. J. and Lorenz M. R.[50] rationalized the role of electrostatic interaction by hypothesising the presence of "contact ion pair" $M^+CO_3^{2-}$ which would be the main contribution to the migration process. We do not see the presence of such "contact ion pair" $M^+CO_3^{2-}$ in the structural solvation structure obtained in our molecular simulation.

Conclusions

This work reports new structural and transport results obtained in two binary systems of carbonates: Li_2CO_3-Na_2CO_3 and Li_2CO_3-K_2CO_3. We have characterized the speciation as a function of composition in both system using an innovate NMR high-temperature measurement. The measured ^{13}C chemical shifts are similar regardless of the type of alkali and correspond to the CO_3^{2-} species in molten carbonates.

In the Li_2CO_3-K_2CO_3 system we note the effect of K_2CO_3 by the linear dependence of the ^{17}O chemical shifts. This change is caused by the structural evolution of K^+ and Li^+ cations around the oxygen.

In addition, we measured the self-diffusion coefficients for both systems, and we did not observe any significant effect of alkalis. These measurements allowed us to highlight the charge transport mechanism by combining Nernst-Einstein relationship and the factor Haven. We found a non-negligible effect of alkali metals on electrical conductivity in molten carbonates. This effect is not related to the cationic radius as suggested in the literature. Moreover, when K_2CO_3 is added in the composition, the interaction between the charge carriers present in the molten salt increases and the electrical conductivity is reduced which would correspond to a major contribution of contact ion pair in the electrical conductivity.

For Li_2CO_3-Na_2CO_3 we observe that the factor Haven is close to 1 for all composition, which means there is no large interactions between the charge carriers. This allows the ions to move more “freely” in the molten carbonates and thus increase the value of conductivity.

A deeper analysis of the transport mechanism would rely on accurate molecular simulations, such work is ongoing in our group.

Corresponding Author

Antonii Zhadan - Conditions Extrêmes et Materiaux: Haute Température et Irradiation, CEMHTI, UPR 3079-CNRS Univ Orleans 45071 Orléans, France; https://orcid.org/0000-0001-7975-4654; Email: antonii.zhadan@cnrs-orleans.fr

Authors

Vincent Sarou-Kanian - Conditions Extrêmes et Materiaux: Haute Température et Irradiation, CEMHTI, UPR 3079-CNRS Univ Orleans 45071 Orléans, France;

Antoine Carof – Laboratoire de Physique et Chimie Théoriques, LPCT, CNRS, Université de Lorraine F-54000 Nancy, France

Leire Del Campo - Conditions Extrêmes et Materiaux: Haute Température et Irradiation, CEMHTI, UPR 3079-CNRS Univ Orleans 45071 Orléans, France;

Lionel Cosson - Conditions Extrêmes et Materiaux: Haute Température et Irradiation, CEMHTI, UPR 3079-CNRS Univ Orleans 45071 Orléans, France;

Rodolphe Vuilleumier - PASTEUR, Département de Chimie, Ecole Normale Supérieur, PSL University, Sorbonne Université, CNRS, 75005, Paris, France

Mohammed Malki - Conditions Extrêmes et Materiaux: Haute Température et Irradiation, CEMHTI, UPR 3079-CNRS Univ Orleans 45071 Orléans, France;

Catherine Bessada - Conditions Extrêmes et Materiaux: Haute Température et Irradiation, CEMHTI, UPR 3079-CNRS Univ Orleans 45071 Orléans, France;

Author Contributions

A.Z. conceptualized and planned the project. A.Z. conducted all of the NMR experiments with assistance from V.S.K. and C.B, with L.D.C. and M.M., L.C. performed the measurements of electrical conductivity, the simulation part with assistance from A.C. and R.V. The manuscript was written with contribution from all coauthors.

Notes

The authors declare no competing financial interest.

ACKNOWLEDGMENT

This work was funded by the French National Research Agency (ANR-17-CE05-0025 project MCEC). Financial support from the IR-RMN-THC FR 3050 CNRS for conducting the research is gratefully acknowledged.

REFERENCES

(1) Cassir, M.; McPhail, S. J.; Moreno, A. Strategies and New Developments in the Field of Molten Carbonates and High-Temperature Fuel Cells in the Carbon Cycle. *Int. J. Hydrogen Energy* **2012**, *37* (24), 19345–19350. https://doi.org/10.1016/j.ijhydene.2011.11.006.

(2) Ijije, H. V.; Chen, G. Z. Electrochemical Manufacturing of Nanocarbons from Carbon Dioxide in Molten Alkali Metal Carbonate Salts: Roles of Alkali Metal Cations. *Adv. Manuf.* **2016**, *4* (1), 23–32. https://doi.org/10.1007/s40436-015-0125-2.

(3) Meléndez-Ceballos, A.; Gürbüz, E.; Brouzgou, A.; Albin, V.; Ringuedé, A.; Lair, V.; Cassir, M. Input on the Measurement and Comprehension of CO_2 Solubility in Molten Alkali Carbonates in View of Its Valorization . *J. Electrochem. Soc.* **2020**, *167* (6), 064504. https://doi.org/10.1149/1945-7111/ab7ce1.

(4) Milewski, J.; Bujalski, W.; Wołowicz, M.; Futyma, K.; Kucowski, J.; Bernat, R. Experimental Investigation of CO_2 Separation from Lignite Flue Gases by 100 cm^2 Single Molten Carbonate Fuel Cell. *Int. J. Hydrogen Energy* **2014**, *39* (3), 1558–1563. https://doi.org/10.1016/j.ijhydene.2013.08.144.

(5) Discepoli, G.; Milewski, J.; Desideri, U. Off-Design Operation of Coal Power Plant Integrated with Natural Gas Fueled Molten Carbonate Fuel Cell as CO_2 Reducer. *Int. J. Hydrogen Energy* **2016**, *41* (8), 4773–4783. https://doi.org/10.1016/j.ijhydene.2016.01.065.

(6) Bonafous, L.; Ollivier, B.; Auger, Y.; Chaudret, H.; Bessada, C.; Massiot, D.; Farnan, I.;

Coutures, J. High Temperature NMR Observation of Mobile Phases up to 1500°C. *J. Chim. Phys.* **1995**, *92* (92), 1867–1870. https://doi.org/10.1051/jcp/1995921867.

(7) Rollet, A. L.; Sarou-Kanian, V.; Bessada, C. Measuring Self-Diffusion Coefficients up to 1500 K: A Powerful Tool to Investigate the Dynamics and the Local Structure of Inorganic Melts. *Inorg. Chem.* **2009**, *48* (23), 10972–10975. https://doi.org/10.1021/ic9010086.

(8) Zhadan, A.; Sarou-Kanian, V.; Del Campo, L.; Cosson, L.; Malki, M.; Bessada, C. Transport Properties in Molten Carbonates: Self-Diffusion and Conductivity Measurements at High Temperature. *Int. J. Hydrogen Energy* **2021**, *46* (28), 15059–15065. https://doi.org/10.1016/j.ijhydene.2020.06.294.

(9) Gaillard, F.; Malki, M.; Iacono-Marziano, G.; Pichavant, M.; Scaillet, B. Carbonatite Melts and Electrical Conductivity in the Asthenosphere. *Science (80-.).* **2008**, *322* (5906), 1363–1365. https://doi.org/10.1126/science.1164446.

(10) Gale, Robert J., Lovering, D. . *Molten Salt Techniques*; Gale, R. J., Lovering, D. G., Eds.; Springer US: Boston, MA, 1984. https://doi.org/10.1007/978-1-4615-7502-3.

(11) Ostrovskaya, N. F.; Bartnitskaya, T. S.; Lyashenko, V. I.; Zelyavskii, V. B.; Kurdyumov, A. V. Crystallization of Boron Nitride from Solution in a Lithium Borate Melt. *Powder Metall. Met. Ceram.* **1996**, *35* (11–12), 636–639. https://doi.org/10.1007/BF01513049.

(12) Gál, S.; Tomor, K.; Pungor, E.; Soóki-Tóth, G.; Horváth, P. Reactions of Binary and Ternary Alkali Metal Carbonate Mixtures with Aluminium Oxide. *J. Therm. Anal.* **1976**, *9* (2), 241–250. https://doi.org/10.1007/BF01909387.

(13) Zhadan, A.; Sarou-kanian, V.; Del Campo, L.; Cosson, L.; Malki, M.; Bessada, C. Speciation and Transport Properties in Molten Alkali Carbonates at High Temperature. *J. Phys. Chem. C* **2022**, *126* (40), 17234–17242. https://doi.org/10.1021/acs.jpcc.2c03048.

(14) Spedding, P. L.; Mills, R. Trace-Ion Diffusion in Molten Alkali Carbonates. *J. Electrochem. Soc.* **1965**, *112* (6), 594–599. https://doi.org/10.1149/1.2423614.

(15) Pommier, A.; Gaillard, F.; Malki, M.; Pichavant, M. Methodological Re-Evaluation of the Electrical Conductivity of Silicate Melts. *Am. Mineral.* **2010**, *95* (2–3), 284–291. https://doi.org/10.2138/am.2010.3314.

(16) Marrocchelli, D.; Salanne, M.; Madden, P. A. High-Pressure Behaviour of GeO_2 : A Simulation Study. *J. Phys. Condens. Matter* **2010**, *22* (15), 152102. https://doi.org/10.1088/0953-8984/22/15/152102.

(17) Vuilleumier, R.; Seitsonen, A.; Sator, N.; Guillot, B. Structure, Equation of State and Transport Properties of Molten Calcium Carbonate ($CaCO_3$) by Atomistic Simulations. *Geochim. Cosmochim. Acta* **2014**, *141*, 547–566. https://doi.org/10.1016/j.gca.2014.06.037.

(18) Salanne, M.; Simon, C.; Turq, P.; Madden, P. A. Conductivity-Viscosity-Structure: Unpicking the Relationship in an Ionic Liquid. *J. Phys. Chem. B* **2007**, *111* (18), 4678–4684. https://doi.org/10.1021/jp067073a.

(19) Salanne, M.; Simon, C.; Groult, H.; Lantelme, F.; Goto, T.; Barhoun, A. Transport in Molten LiF–NaF–ZrF_4 Mixtures: A Combined Computational and Experimental Approach. *J. Fluor. Chem.* **2009**, *130* (1), 61–66.

https://doi.org/10.1016/j.jfluchem.2008.07.005.

(20) Merlet, C.; Madden, P. A.; Salanne, M. Internal Mobilities and Diffusion in an Ionic Liquid Mixture. *Phys. Chem. Chem. Phys.* **2010**, *12* (42), 14109–14114. https://doi.org/10.1039/c0cp01412e.

(21) Araque, J. C.; Yadav, S. K.; Shadeck, M.; Maroncelli, M.; Margulis, C. J. How Is Diffusion of Neutral and Charged Tracers Related to the Structure and Dynamics of a Room-Temperature Ionic Liquid? Large Deviations from Stokes–Einstein Behavior Explained. *J. Phys. Chem. B* **2015**, *119* (23), 7015–7029. https://doi.org/10.1021/acs.jpcb.5b01093.

(22) Salanne, M.; Simon, C.; Turq, P.; Heaton, R. J.; Madden, P. A. A First-Principles Description of Liquid BeF_2 and Its Mixtures with LiF: 2. Network Formation in LiF−BeF_2. *J. Phys. Chem. B* **2006**, *110* (23), 11461–11467. https://doi.org/10.1021/jp061002u.

(23) Carof, A.; Coudert, F.-X.; Corradini, D.; Lesnicki, D.; Desmaele, E.; Vuilleumier, R. Carbon Species Solvated in Molten Carbonate Electrolyser Cell from First-Principles Simulations. *Int. J. Hydrogen Energy* **2021**, *46* (28), 15008–15023. https://doi.org/10.1016/j.ijhydene.2020.10.022.

(24) Janssen, G. J. M.; Tissen, J. T. W. M. Pair Potentials from Ab Initio Calculations for Use in Md Simulations of Molten Alkali Carbonates. *Mol. Simul.* **1990**, *5* (1–2), 83–98. https://doi.org/10.1080/08927029008022410.

(25) Tissen, J. T. W. M.; Janssen, G. J. M. Molecular-Dynamics Simulation of Molten Alkali

Carbonates. *Mol. Phys.* **1990**, *71* (2), 413–426. https://doi.org/10.1080/00268979000101871.

(26) Tissen, J. T. W. M.; Janssen, G. J. M.; Eerden, P. van der. Molecular Dynamics Simulation of Binary Mixtures of Molten Alkali Carbonates. *Mol. Phys.* **1994**, *82* (1), 101–111. https://doi.org/10.1080/00268979400100084.

(27) Costa, M. F. Molecular Dynamics of Molten Li_2CO_3-K_2CO_3. *J. Mol. Liq.* **2008**, *138* (1–3), 61–68. https://doi.org/10.1016/j.molliq.2007.08.001.

(28) Corradini, D.; Coudert, F. X.; Vuilleumier, R. Insight into the Li_2CO_3-K_2CO_3 Eutectic Mixture from Classical Molecular Dynamics: Thermodynamics, Structure, and Dynamics. *J. Chem. Phys.* **2016**, *144* (10). https://doi.org/10.1063/1.4943392.

(29) Desmaele, E.; Sator, N.; Vuilleumier, R.; Guillot, B. Atomistic Simulations of Molten Carbonates: Thermodynamic and Transport Properties of the Li_2CO_3 - Na_2CO_3 - K_2CO_3 System. *J. Chem. Phys.* **2019**, *150* (9), 094504. https://doi.org/10.1063/1.5082731.

(30) Desmaele, E.; Sator, N.; Vuilleumier, R.; Guillot, B. The $MgCO_3$ - $CaCO_3$ - Li_2CO_3 - Na_2CO_3 - K_2CO_3 Melts: Thermodynamics and Transport Properties by Atomistic Simulations. *J. Chem. Phys.* **2019**, *150* (21), 214503. https://doi.org/10.1063/1.5099015.

(31) Kiyobayashi, T.; Kojima, T.; Ozaki, H.; Kiyohara, K. Ionic Conductivity of Molten Alkali-Metal Carbonates A_2CO_3 (A = Li, Na, K, Rb, and Cs) and Binary Mixtures $(Li_{1-x}Cs_x)_2CO_3$ and $(Li_{1-x}K_x)_2CO_3$: A molecular dynamics simulation. *J. Chem. Phys.* **2019**, *151* (7), 074503. https://doi.org/10.1063/1.5109912.

(32) Feng, T.; Yang, B.; Lu, G. Deep Learning-Driven Molecular Dynamics Simulations of Molten Carbonates: 1. Local Structure and Transport Properties of Molten Li_2CO_3-Na_2CO_3 System. *Ionics (Kiel).* **2022**, *28* (3), 1231–1248. https://doi.org/10.1007/s11581-021-04429-8.

(33) Machado, K.; Zanghi, D.; Sarou-Kanian, V.; Cadars, S.; Burbano, M.; Salanne, M.; Bessada, C. Study of NaF-AlF_3 Melts by Coupling Molecular Dynamics, Density Functional Theory, and NMR Measurements. *J. Phys. Chem. C* **2017**, *121* (19), 10289–10297. https://doi.org/10.1021/acs.jpcc.7b01530.

(34) Rollet, A. L.; Sarou-Kanian, V.; Bessada, C. Self-Diffusion Coefficient Measurements at High Temperature by PFG NMR. *Comptes Rendus Chim.* **2010**, *13* (4), 399–404. https://doi.org/10.1016/j.crci.2009.11.005.

(35) Jerschow, A.; Müller, N. Suppression of Convection Artifacts in Stimulated-Echo Diffusion Experiments. Double-Stimulated-Echo Experiments. *J. Magn. Reson.* **1997**, *125* (2), 372–375. https://doi.org/10.1006/jmre.1997.1123.

(36) Simonneta, C.; Phalippou, J.; Malki, M.; Grandjean, A. Electrical Conductivity Measurements of Oxides from Molten State to Glassy State. *Rev. Sci. Instrum.* **2003**, *74* (5), 2805–2810. https://doi.org/10.1063/1.1564272.

(37) Miyazaki, Y.; Yanagida, M.; Tanimoto, K.; Kodama, T.; Tanase, S. An Apparatus for Electrical Conductance Measurements with Molten Carbonates. *J. Electrochem. Soc.* **1986**, *133* (7), 1402–1404. https://doi.org/10.1149/1.2108897.

(38) Lair, V.; Albin, V.; Ringuedé, A.; Cassir, M. Theoretical Predictions vs. Experimental

Measurements of the Electrical Conductivity of Molten Li_2CO_3–K_2CO_3 Modified by Additives. *Int. J. Hydrogen Energy* **2012**, *37* (24), 19357–19364. https://doi.org/10.1016/j.ijhydene.2011.09.153.

(39) Kojima, T.; Miyazaki, Y.; Nomura, K.; Tanimoto, K. Electrical Conductivity of Molten Li_2CO_3-X_2CO_3 (X: Na, K, Rb, and Cs) and Na_2CO_3-Z_2CO_3 (Z: K, Rb, and Cs). *J. Electrochem. Soc.* **2007**, *154* (12), 222–230. https://doi.org/10.1149/1.2789389.

(40) Parrinello, M.; Rahman, A. Polymorphic Transitions in Single Crystals: A New Molecular Dynamics Method. *J. Appl. Phys.* **1981**, *52* (12), 7182–7190. https://doi.org/10.1063/1.328693.

(41) Martyna, G. J.; Tobias, D. J.; Klein, M. L. Constant Pressure Molecular Dynamics Algorithms. *J. Chem. Phys.* **1994**, *101* (5), 4177–4189. https://doi.org/10.1063/1.467468.

(42) Shinoda, W.; Shiga, M.; Mikami, M. Rapid Estimation of Elastic Constants by Molecular Dynamics Simulation under Constant Stress. *Phys. Rev. B - Condens. Matter Mater. Phys.* **2004**, *69* (13), 16–18. https://doi.org/10.1103/PhysRevB.69.134103.

(43) Plimpton, S. Fast Parallel Algorithms for Short-Range Molecular Dynamics. *J. Comput. Phys.* **1995**, *117* (1), 1–19. https://doi.org/10.1006/jcph.1995.1039.

(44) Thompson, A. P.; Aktulga, H. M.; Berger, R.; Bolintineanu, D. S.; Brown, W. M.; Crozier, P. S.; in 't Veld, P. J.; Kohlmeyer, A.; Moore, S. G.; Nguyen, T. D.; Shan, R.; Stevens, M. J.; Tranchida, J.; Trott, C.; Plimpton, S. J. LAMMPS - a Flexible Simulation Tool for Particle-Based Materials Modeling at the Atomic, Meso, and Continuum Scales. *Comput. Phys. Commun.* **2022**, *271*, 108171. https://doi.org/10.1016/j.cpc.2021.108171.

(45) Desmaele, E.; Sator, N.; Vuilleumier, R.; Guillot, B. Atomistic Simulations of Molten Carbonates: Thermodynamic and Transport Properties of the Li_2CO_3 - Na_2CO_3 - K_2CO_3 System. *J. Chem. Phys.* **2019**, *150* (9), 094504. https://doi.org/10.1063/1.5082731.

(46) Ewald, P. P. Die Berechnung Optischer Und Elektrostatischer Gitterpotentiale. *Ann. Phys.* **1921**, *369* (3), 253–287.

(47) Dunstan, M. T.; Griffin, J. M.; Blanc, F.; Leskes, M.; Grey, C. P. Ion Dynamics in Li2CO3 Studied by Solid-State NMR and First-Principles Calculations. *J. Phys. Chem. C* **2015**, *119* (43), 24255–24264. https://doi.org/10.1021/acs.jpcc.5b06647.

(48) Marchenko, A.; Truflandier, L. A.; Autschbach, J. Uranyl Carbonate Complexes in Aqueous Solution and Their Ligand NMR Chemical Shifts and ^{17}O Quadrupolar Relaxation Studied by Ab Initio Molecular Dynamics. *Inorg. Chem.* **2017**, *56* (13), 7384–7396. https://doi.org/10.1021/acs.inorgchem.7b00396.

(49) Mills, R.; Spedding, P. L. An Interpretation of the Concentration Dependence of Mobilities in Fused Alkali Carbonate Mixtures. *J. Phys. Chem.* **1966**, *70* (12), 4077–4079. https://doi.org/10.1021/j100884a507.

(50) Janz, G. J.; Lorenz, M. R. Molten Carbonate Electrolytes: Physical Properties, Structure, and Mechanism of Electrical Conductance. *J. Electrochem. Soc.* **1961**, *108* (11), 1052. https://doi.org/10.1149/1.2427946.

(51) Spedding, P. L.; Mills, R. Tracer Diffusion Measurements in Mixtures of Molten Alkali Carbonates. *J. Electrochem. Soc.* **1966**, *113* (6), 599–603. https://doi.org/10.1149/1.2424035.

(52) Näfe, H. Conductivity of Alkali Carbonates, Carbonate-Based Composite Electrolytes and IT-SOFC. *ECS J. Solid State Sci. Technol.* **2014**, *3* (2), N7–N14. https://doi.org/10.1149/2.015402jss.

(53) Kojima, T.; Miyazaki, Y.; Nomura, K.; Tanimoto, K. Physical Properties of Molten Li_2CO_3-Na_2CO_3 (52:48 Mol%) and Li_2CO_3-K_2CO_3 (62:38 Mol%) Containing Additives. *J. Electrochem. Soc.* **2013**, *160* (10), H733–H741. https://doi.org/10.1149/2.073410jes.

(54) Janz, G. J.; Volume, M. S.; Mixed, P.; Melts, H.; Conductance, E.; Janz, G. J. Molten Salts Data as Reference Standards for Density , Surface Tension , Viscosity , and Electrical Conductance : KNO_3 and NaCl Published by the AIP Publishing Articles You May Be Interested in Molten Salts Data as Reference Standards for Density , Surfac. **1980**, *3*. https://doi.org/10.1063/1.555634.

(55) Janz, G. J.; Tomkins, R. P. T. Molten Salts: Vol. 5, Part 1, Additional Single and Multi-Component Salt Systems. Electrical Conductance, Density, Viscosity, and Surface Tension Data. *J. Phys. Chem. Ref. Data* **1980**, *9* (4), 831–1022. https://doi.org/10.1063/1.555635.

(56) Kojima, T.; Miyazaki, Y.; Nomura, K.; Tanimoto, K. Electrical Conductivity of Molten Li_2CO_3–X_2CO_3 (X: Na, K, Rb, and Cs) and Na_2CO_3–Z_2CO_3 (Z: K, Rb, and Cs). **2007**, *3*, 222–230. https://doi.org/10.1149/1.2789389.

Table of Contents

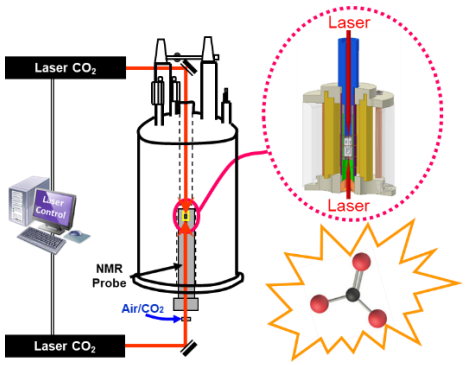

SYNOPSIS

Speciation and transport properties in molten alkali carbonates in Li_2CO_3-Na_2CO_3 and Li_2CO_3-K_2CO_3 binary systems at high temperature were investigated using a combination of high temperature NMR, pulse field gradient NMR, electrical impedancemetry and classical (force field-based) molecular dynamics simulation. Electrostatic interactions in molten carbonates are observed and discussed.